Complexity Beyond Steady State in Coupled Two-Mode Lasers

Muhammad Abdul[*1], Umar F. Zubairy[2], Farhan Saif[3]

Quantum Electronics Labs., Department of Electronics, Quaid-I-Azam University Islamabad 3rd Av., 45320, Pakistan

[*1]mabdul_qau@yahoo.com; [3]Farhan.saif@fulbrightmail.org

***Abstract*- One dimensional laser logistic map is derived from semi-classical theory of single mode laser and discussed. Later, we write lasers in a ring cavity, with a system of two maps symmetrically coupled. The theoretical system reveals complicated dynamics. We investigated bifurcation phenomenon and crises behavior for the system.**

Keywords- Discrete Maps; Instability Behaviour of Strange Attractor; Bifurcation

I. INTRODUCTION

Willis E. Lamb, in 1964, presented semi-classical theory of lasers in homogeneously broadened media [1]. In later years, an analogy between semi-classical lasers and Lorentz model for incompressible fluid dynamics was introduced by Herman Haken [2]. Based on Maxwell-Bloch equation, Haken's proposition was considered a foundation stone to explain nonlinear evolution in laser. However, it was observed that in this proposition the required laser parameters correspond to bad cavity limit, that is, cavity decay time is considerably larger than atomic decay time. In other laser models, a periodic solutions have been found for single-mode lasers with either a constant [3] or modulated [4] external field for laser parameters, and for optically pumped three level lasers [5]. One-dimensional maps are useful models not only for the description of specific population evolution but also as a kind of stroboscopic representation of the continuous solutions of nonlinear differential equations [6]. The competition between two species has already been discussed in the literature in term of coupled first order equations of form similar to that governing the single species growth [7]. In this paper, we explain two-mode ring lasers as a function of coupling strength, as the given equations reduce to coupled first order equations [8, 9]. In coupled logistic maps, we found self-similarity stripe structure of basins, distortion of torus and transition to chaos [10]. Since, there are two types of coupling linear and bilinear coupling. Both have its own importance but here we are studying bilinear coupling. Coupled oscillators are very important in nonlinear dynamics and for its developments from classic problems of coupled lasers, electronics oscillators to biological model [11]. Localized synchronization is observed in two coupled but non-identical semiconductor lasers [12]. Coupled logistic maps exhibit complicated dynamical behavior, including quasi-periodicity, period adding, phase locking, intermittency, long-lived, and chaotic transients, etc.

II. EINSTEIN MAXWELL'S EQUATIONS

We consider excited atoms placed inside a cavity in a ring configuration. Mirrors 1 and 2 have reflectivity R, while mirrors 3 and 4 have hundred percent reflectivity, so that the reflected amplified light is back to interact with the atoms. Phenomenologically laser process takes place as light interacts with the material atoms that emit identical radiations, the phenomena continues.

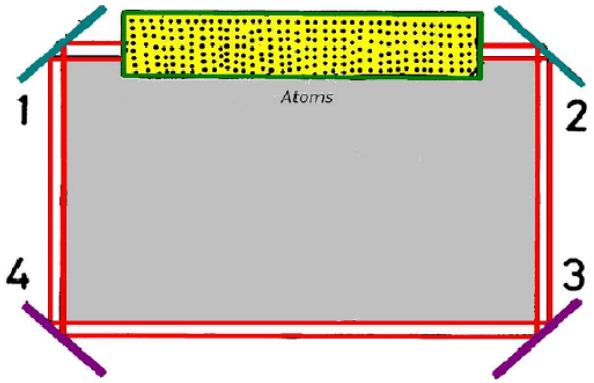

Fig. 1 Ring cavity in which EMT wave is propagating in one direction

Since mirrors R_1 and R_2 have reflectivity less than hundred percent, some of photons are transmitted out of the cavity. We consider the interaction of a single-mode radiation field of frequency ν with a two-level Schrödinger atom [13, 14], and label the two state $|a\rangle$ and $|b\rangle$, indicating the excited and ground state respectively. We take H_0 as the atomic Hamiltonian so that both state $|a\rangle$ and $|b\rangle$ are its eigenstate state with $\hbar\omega_a$ and $\hbar\omega_b$ as the corresponding eigen-energies. Therefore, by using the

completeness relation, |a⟩⟨a|+|b⟩⟨b|=1, the Hamiltonian of the LS is defined as the sum of atomic Hamiltonian and Hamiltonian describing the interaction of the atom with the e.m. field, that is,

$$H = \hbar\omega_a |a\rangle\langle a| + \hbar\omega_b |b\rangle\langle b| - (\wp_{ab} |a\rangle\langle b| + \wp_{ba} |b\rangle\langle a|)E(t). \quad (1)$$

Where $\wp_{ab}=\wp_{ba}^* = e\langle a|x|b\rangle$ is the matrix element of the electric dipole moment and, E(t) is the field at the atom. The equations of motion for the density matrix elements, ρ_{ij}, are given as,

$$\begin{aligned} \dot{\rho}_{aa} &= \lambda_a - \Upsilon_a \rho_{aa} + \frac{i}{\hbar}[\wp E \rho_{ba} - c.c], \\ \dot{\rho}_{bb} &= \lambda_b - \Upsilon_b \rho_{bb} - \frac{i}{\hbar}[\wp E \rho_{ba} - c.c], \\ \dot{\rho}_{ab} &= -(i\omega + \Upsilon)\rho_{ab} - \frac{i}{\hbar}\wp E(\rho_{aa} - \rho_{bb}], \end{aligned} \quad (2)$$

where ρ_{aa} , and ρ_{bb} express the probability of finding the atom in excited state, ground state and transition from ground to excited state respectively. Here, Υ_a and Υ_b are the decay rates associated to level ***a*** and ***b***. Furthermore $\lambda_a = \Upsilon_a \rho_{aa}^{(0)}$ and $\lambda_b = \Upsilon_b \rho_{bb}^{(0)}$ are constant rate at which atoms are being pumped from level ***b*** to upper level ***a***. The electric field is linearly polarized in the cavity and electromagnetic field radiation is described by following Maxwell's equation;

$$-\frac{\partial^2 E}{\partial z^2} + \mu_0\sigma\frac{\partial E}{\partial t} + \frac{1}{c^2}\frac{\partial^2 E}{\partial t^2} = -\mu_0\frac{\partial^2 P}{\partial t^2}, \quad (3)$$

where , μ_0, σ and c are the permeability, conductivity and speed of light respectively. The macroscopic polarization P acts as a source term in the equation for radiation field. The variation in the field intensity transverse to the laser axis is typically slowly varying on the scale of optical wave length, and for the reason, we neglect the *x* and *y* dependence of E, i. e, **E**(*r, t*) = E(z, t)x, polarized along *x*-axis. Hence, the field of frequency ν is represented as,

$$\mathrm{E}(z,t) = \frac{1}{2}\varepsilon(z,t)e^{-i[\nu t - kz + \phi(z,t)]}, \quad (4)$$

where amplitude $\varepsilon(z,t)$ and phase φ(z, t) are slowly varying functions of position and time. The corresponding response of the medium, neglecting the higher harmonics, is given by the macroscopic polarization,

$$\mathrm{P}(z,t) = \frac{1}{2}\wp(z,t)e^{-i[\nu t - kz + \phi(z,t)]}. \quad (5)$$

Here $\wp(z,t)$ is a slowly varying function of position and time, which may be expressed in terms of the population matrix as,

$$\wp(z,t) = \frac{1}{2}\wp\rho_{ab}(z,t)e^{-i[\nu t - kz + \phi(z,t)]}. \quad (6)$$

We apply the slowly varying amplitudes and phase approximation [15, 16]. Substituting field and macroscopic polarization Eqs. (4) and (5) in Eq. (3) and equating real and imaginary parts,

$$\begin{aligned} \frac{\partial\varepsilon}{\partial z} + \frac{1}{c}\frac{\partial\varepsilon}{\partial t} &= -k\varepsilon - \frac{1}{2\in_0}k\,\mathrm{Im}\,\wp, \\ \frac{\partial\varphi}{\partial z} + \frac{1}{c}\frac{\partial\varphi}{\partial t} &= k - \frac{\nu}{c} - \frac{1}{2\in_0}k\,\mathrm{Re}\,\wp, \end{aligned} \quad (7)$$

where $k = \frac{\sigma}{2\in_0 c}$ is linear loss coefficient. We determine the driving polarization Im*P*(*t*) using Eq. (6) in Eq. (2) and on simplifying we get,

$$I_m P(t) = \frac{-\wp^2}{\hbar}E(t)\Upsilon\frac{\rho_{aa}(t) - \rho_{bb}(t)}{\Upsilon^2 + (\omega - \nu)^2}. \quad (8)$$

By substituting the expression in equations (2) and (3), in the steady state ($\dot{\rho}_{aa} = \dot{\rho}_{bb} = 0$), we find

$$\rho_{aa} - \rho_{bb} = \frac{N_0}{1 + R/R_s}, \tag{9}$$

$R = \frac{1}{2}(\frac{\wp\,\varepsilon}{\hbar})^2 \frac{\Upsilon}{\Upsilon + (\omega - \nu)^2}$ is the rate constant, which determines the rate at which the population difference varies in time, $N_0 = \lambda_a \Upsilon_a^{-1} - \lambda_b \Upsilon_b^{-1}$ and $R_s = \Upsilon_a \Upsilon_b / 2\Upsilon$. Therefore, the population difference is directly proportional to N_0 which appears in the absence of field and inversely proportional to the intensity. On substituting Eqs. (8) and (9) in Eq. (7), the equation of motion for the field amplitude becomes,

$$\begin{aligned} \dot{\varepsilon} &= -\frac{C}{2}\varepsilon + \frac{A\varepsilon}{2[1 + \frac{A}{B}(\frac{\in_0 V}{2\hbar\nu})\varepsilon^2]} \\ A &= (\frac{\wp^2 \nu \Upsilon}{\in_0 \hbar}) \frac{N_0}{\Upsilon^2 + (\omega - \nu)^2} \\ B &= (\frac{4\wp^2}{\hbar^2})(\frac{\Upsilon^2}{\Upsilon_a \Upsilon_b}) \frac{A}{\Upsilon^2 + (\omega - \nu)^2} (\frac{\hbar\nu}{2 \in_0 V}). \end{aligned} \tag{10}$$

Here A, B and C, are the Einstein gain coefficient, nonlinear saturation and losses in the system respectively and *V* is the volume of the cavity. We define a dimensionless intensity $n = \frac{\in_0 \varepsilon^2 V}{2\hbar\nu}$, which corresponds to number of photons in the laser field. By substituting in Eq. (10) the laser equation responsible for the intensity growth,

$$\dot{n} = \frac{An}{1 + \frac{B}{A}n} - Cn. \tag{11}$$

Similar rate equation is obtained by quantum theory as we consider the interaction of single-mode quantized field of frequency ν with two level atoms. The probability of *n* photons in the field is obtained by using equation of motion for the laser field density matrix in the presence of interaction with active lasing medium and damping mechanism is

$$\begin{aligned} \dot{P}(n) = &-[\frac{(n+1)A}{1 + (n+1)(\frac{B}{A})}]P(n) + \\ &[\frac{nA}{1 + n(\frac{B}{A})}]P(n-1) - CnP(n) \\ &+ C(n+1)P(n+1). \end{aligned} \tag{12}$$

Where $A = \frac{2\Upsilon_a g^2}{\Upsilon^2}$, and $B = \frac{4g^2}{\Upsilon^2}A$ as discussed above. We derive an equation for the mean number of photons, $\langle n \rangle$ from above equation,

$$\frac{d\langle n \rangle}{dt} = \sum_{n=1}^{n=\infty} n\,\dot{P}(n), \tag{13}$$

which yields,

$$\frac{d\langle n \rangle}{dt} = \sum_{n=1}^{n=\infty} \frac{(n+1)AP(n)}{1 + (1+n)B/A} - C\langle n \rangle. \tag{14}$$

and explain the evolution of mean number of photons in the lasing cavity. Following quantum mechanical treatment to single mode LS [15, 16] we obtain,

$$\dot{\langle n \rangle} = (A - C)\langle n \rangle - B\langle (n+1)^2 \rangle + A. \tag{15}$$

We proceed further under the condition of large average photon number, *i.e*, $\langle n \rangle > 1$ and decorrelation approximation and which implies $\langle n^2 \rangle \approx \langle n \rangle^2$.

III. LASER LOGISTIC MAPPING

We analyze the nonlinear evolution of laser light, in semiclassical and quantum mechanical domains, by developing mapping. Equation (11), obtained by semi-classical theory, lead us to develop laser logistic map (LLM) by expanding the denominator using Taylor's series expansion,

$$\dot{n} = Cn + An[1 - \frac{B}{A}n] + f(n), \tag{16}$$

where $f(n) = An[\frac{B^2}{A^2}n^2 - \frac{B^3}{A^3}n^3 + \frac{B^4}{A^4}n^4 - .....]$ is the sum of higher order terms. If $\Omega_R^2 \square \Upsilon_a \Upsilon_b$, we ignore the higher powers of $\frac{Bn}{A}$, and obtain

$$\dot{n} = (A - C)n[1 - (\frac{B}{A - C})n]. \tag{17}$$

Rescaling the equation by introducing steady state solution, $n_0 = \frac{A - C}{B}$

$$\frac{dN}{dt} = \gamma_0 N(1 - N), \tag{18}$$

where $\gamma_0 = A - C$. Using ab-initio method, left-hand-term in difference form is,

$$\frac{dN}{dt} = \frac{N_{j+1} - N_j}{t_{j+1} - t_j} = \frac{N_{j+1} - N_j}{\Delta t}. \tag{19}$$

Where N_j defines the number of photons at the onset of jth cycle, and N_{j+1} is the number of photons at the onset of next (j + 1)th cycle, *i.e.*, after one round trip time, Δt, of the field in the ring cavity.

$$N_{j+1} = \gamma N_j[1 - N_j] + N_j. \tag{20}$$

Where $\gamma = (A - C)\Delta t$ is dimensionless effective gain coefficient that acts as the controlling parameter of the laser system. Using Eq. (15) obtained by quantum mechanical laser theory, we arrive at the same laser logistic map. Laser threshold condition takes place at $\gamma = 0$, which implies that the gain is balanced by the cavity losses, thus no amplification takes place. On increasing effective gain coefficient γ laser logistic map displays different behavior: (1) For $0 < \gamma < 2$ the iteration converges to value $N_\infty = 1$. This asymptotic value is independent of initial value and corresponds to steady state value of laser. (2) For $2 < \gamma < 2.449$ the iteration alternatively changes between two values, which implies that there are two field intensities available within the cavity corresponding to the γ values from above mentioned domain. (3) For $\gamma > 2.6$ the iteration never settles into any pattern and stays aperiodical. As γ increases beyond 2.6 the light intensity displays a chaotic behavior as a function of j which determines interaction time. We have discussed stable, bistable, multi-bistable and chaotic laser in a ring cavity using convergent, cyclic and chaotic solution of LLM. The evolution of the LLM, given in Eq. (20), is explained both analytically and numerically in our present discussion.

IV. TWO-MODE COUPLED LASERS

We consider a two-mode ring cavity in which waves are propagated in clockwise and counter-clockwise directions around the ring [17, 18], as shown in the Fig. 2.

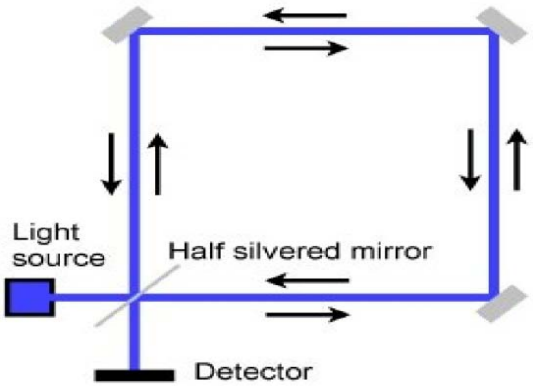

Fig. 2 The possible diagram of ring cavity in which two waves are propagating in clockwise and anti-clockwise direction

Mathematical formulation and simplification of these two-mode traveling waves in the cavity has been calculated [1, 19]. These equations, written for electric field E_1 and E_2 are also called nonlinear coupled laser dynamical equation,

$$\frac{dE_1}{dt} = [A - C_1 - B(|E_1|^2 + \xi |E_2|^2)]E_1,$$
$$\frac{dE_1}{dt} = [A - C_2 - B(|E_2|^2 + \xi |E_1|^2)]E_2, \tag{21}$$

where ξ is given as,

$$\xi = \frac{1}{[1 + (\Delta\omega T_1)^2]}, \tag{22}$$

where T_1 is natural life time of laser transitions, and $\Delta\omega$ is detuning [19]. We multiply $2E_1^*$ and $2E_2^*$ to Eq. (21). Later a simplification and normalization with $(\frac{B}{(A-C_i)})^{-1}$, which is steady state photon number, leads us to obtain the difference equations,

$$x_{n+1} = x_n + 2\lambda_1 x_n[1 - (x_n + \xi y_n)],$$
$$y_{n+1} = y_n + 2\lambda_2 y_n[1 - (y_n + \xi x_n)]. \tag{23}$$

We obtain the difference equations using ab-initio method, that is, $\frac{dx}{dt} = \frac{x_{j+1} - x_j}{\Delta t}$. Furthermore, we take $(A - C_i)\Delta t = \lambda_i$ as the controlling parameter, and $\Delta t = t^+ - t^-$ is the cavity round trip time. Here t^+ and t^- are times of the waves which are propagating clockwise and anticlockwise directions respectively. Equation (23) provides the set of coupled logistic maps, and shall be discussed in detail in next section with ξ as real.

V. TWO-MODE COUPLED LASERS

The dynamical system described here which serves as a distinct concept for an entrainment behavior between the strange attractors of coupled nonlinear oscillators. In general in the absence of coupling, each behaves like a single longitudinal and transverse mode [10, 12]. We find that there is a certain range of coupling strength for which synchronized chaos exists. Beyond this range of coupling strength synchronization breaks down, and the system enters a regime of turbulence or spatiotemporal chaos [9, 13]. Hence, we report that in two-mode ring lasers, synchronization oscillates between quasi-periodic, intermittency state, period bifurcation and chaoticity, by fixing controlling parameter and changing the coupling strength. Here, we also discuss period fusing and emerging because of crises where strange attractors fluctuate corresponding to the change of parameters. We may write the coupled logistic equations as [24],

$$x_{n+1} = F(x_n, y_n) = x_n + 2\lambda_1 x_n(1 - x_n) - \gamma y_n x_n,$$
$$y_{n+1} = F(x_n, y_n) = y_n + 2\lambda_2 y_n(1 - y_n) - \gamma y_n x_n, \tag{24}$$

where, λ_i and $\gamma = 2\lambda_i\xi$, (i = 1; 2) are the characteristic parameters, therefore, the system is controlled by mean of three parameters. A mapping of bilinear and linear coupling terms have been shown to exhibit complicated dynamical behavior including quasi periodicity, phase locking, intermittency, period adding, long-lived chaotic transitions and then periodicity [25, 26]. Following we explain necessary terms and their symbols used in our later discussion.

Fixed points: A fixed point x is a point in the space defined by function f, so that $f_n(x) = x \ \forall \ n$.

Periodic motion: A periodic motion (P) of a system is defined as $f_n(x) = f_{n+1}(x)$.

Quasi-periodic motion: A Quasi-periodic motion (QP) of a dynamical system is defined as $f : R \to R^n$; dynamical function can be represented in the form $f = H(\omega_1, \omega_2, \omega_3, ...\omega_n)$; where H is periodic with period 2π in each argument, and the real numbers $(\omega_1, \omega_2, \omega_3, ...\omega_n)$ describe the finite set of base frequencies [27, 28].

Phase locking: The process of phase locking exists whenever the chaotic actions of the individual subsystems shift to the ordered actions of the collective system [29, 30]. Sometimes phase entrainment is called phase locking.

Chaotic motion: In the chaotic system, there occurs sensitive dependence to initial conditions, i. e, chaotic trajectories locally diverge away from each other and small changes in starting conditions build up exponentially fast into large deviations in the evolution [31].

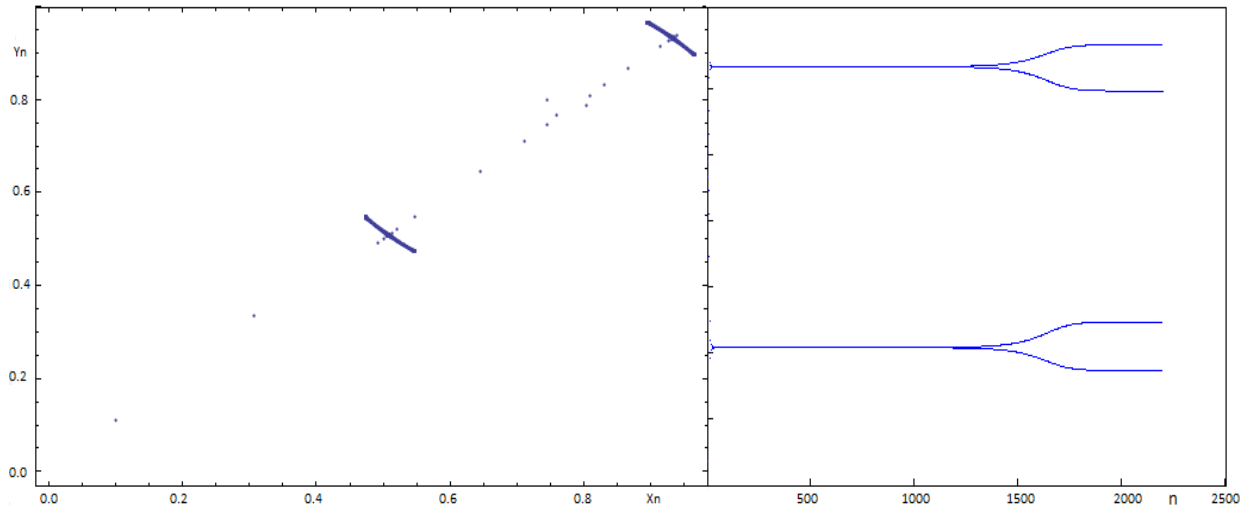

Fig. 3 Phase space (x_n, y_n) is plotted by solving Eq. (24) for $\lambda_1 = \lambda_2 = 1.19$ and $\gamma = 0.660$. We note that the system displays a 4P to 2P behavior through period bifurcation by means of crises. In the plot on right hand side, we present y axis of the phase space as a function of number of iterations. The possible diagram of ring cavity in which two waves are propagating in clockwise and anti-clockwise direction

There occurs a fascinating behavior of the coupled equations (24) for various values of λ_i and γ. The key to understand the structure of these equations in xy-space is a careful analysis of fixed points of the mapping functions as well as their iterates. Since the function $f^{(1)}$ and $f^{(2)}$ are symmetrical, we expect symmetrical behavior in x and y. The two fixed points [32], corresponding to Eq. (26) are,

$$x_1^{(1)} = 0 \sim\sim\sim and \sim\sim\sim x_2^{(1)} = \frac{2\gamma - 2\lambda_1}{(\gamma^2 / \lambda_2 - 4\lambda_1)}.$$

These are stable if they follow the condition,

$$\left\| \frac{dx_{n+1}}{dx_n} - \frac{dx_{n+1}}{dy_n} \right\| \angle 1.$$

In case these fixed points become,

$$x_1^{(1)} = 0 \sim\sim\sim and \sim\sim\sim x_2^{(1)} = \frac{1}{(\gamma / 2\lambda - 1)}.$$

which overlap for $\lambda_i = 0$. By fixing λ_i and varying γ we have found evidence for a boundary crises in our system, like or similar to what was found in Henon's maps by Grebogi, Ott and Yorke [26, 33]. A boundary crisis occurs in our case through the collision of a chaotic attractor with the basin boundaries that separate it from the several other coexistent periodic attractors, in addition with another chaotic attractor [34, 35]. An increase of beyond its critical value for the onset of crises, results in disappearance of the chaotic attractors and its basin while the basins of remaining attractors undergo a sudden expansion.

We report chaotic behavior in our system corresponding to various values of the parameters. We explain the behavior and classify our discussion in two cases: In the first case we fix λ_i and vary γ over a range of $0.001 \le \gamma \le 0.999$ for $x_0 = 0.1$ and $y_0 = 0.11$ [27, 28]. At $\lambda_i = 0.25$ the trajectory in phase space (x; y) converges to a fixed point. The asymptotic character of the solution is typical 1P. For $\lambda_i = 1.0$, system shows oscillatory behavior between QP and 2P character upto $\gamma = 0.999$. There is still 2P character for $\lambda_i = 1.19$ and in the interval $\gamma \in [0.001, 0.21]$. At the upper range of this interval, it shows QP 2 Torus, 4P and 2P respectively at $\gamma = 0.22, 0.222, 0.6851$. Periodic bifurcation phenomena at $\gamma = 0.660$ is also observed, as shown in the Fig. 3. There is no chaotic behaviors seen but our coupled system oscillates between 2P to 4P through quasi-periodicity. It is clear that if coupling strength is increased periodicity fuses and comes out of the crises, finally we get period 2 at $\gamma = 0.999$.

For $\lambda_i = 1.25$ and $\gamma = 0.001$ the four chaotic attractors grow as coupling strength increases. They are synchronized (mirror image of each other) as well as orthogonal, and the trajectory in phase space converges to 4P. When $\gamma = 0.1750$ transition from 4P to 8P takes place, which shows quasi periodicity in which each attractor displays curious nine wing pattern before settling to the asymptotic 8P state. They also fluctuate and expand at $\gamma = 0.1790$ which generates mirror image of laser attractors. At $\gamma = 0.1845$,

transient solution again shows curious nine wing pattern before going to periodic regime. At $\gamma = 0.2$ the lasing system shows chaotic behavior through QP and laser attractors in phase space have exact mirror image of each other, as shown in Fig. 4(a,b). In laser chaos there exists inner crisis, a boundary crisis where a strange attractor collides with unstable fixed points on the boundary of basin of attraction, causing disappearance of both [36, 33]. But in our case when they collide unstable fixed points disappear and shape of the strange attractor remains invariant that becomes unstable as parameters increase.

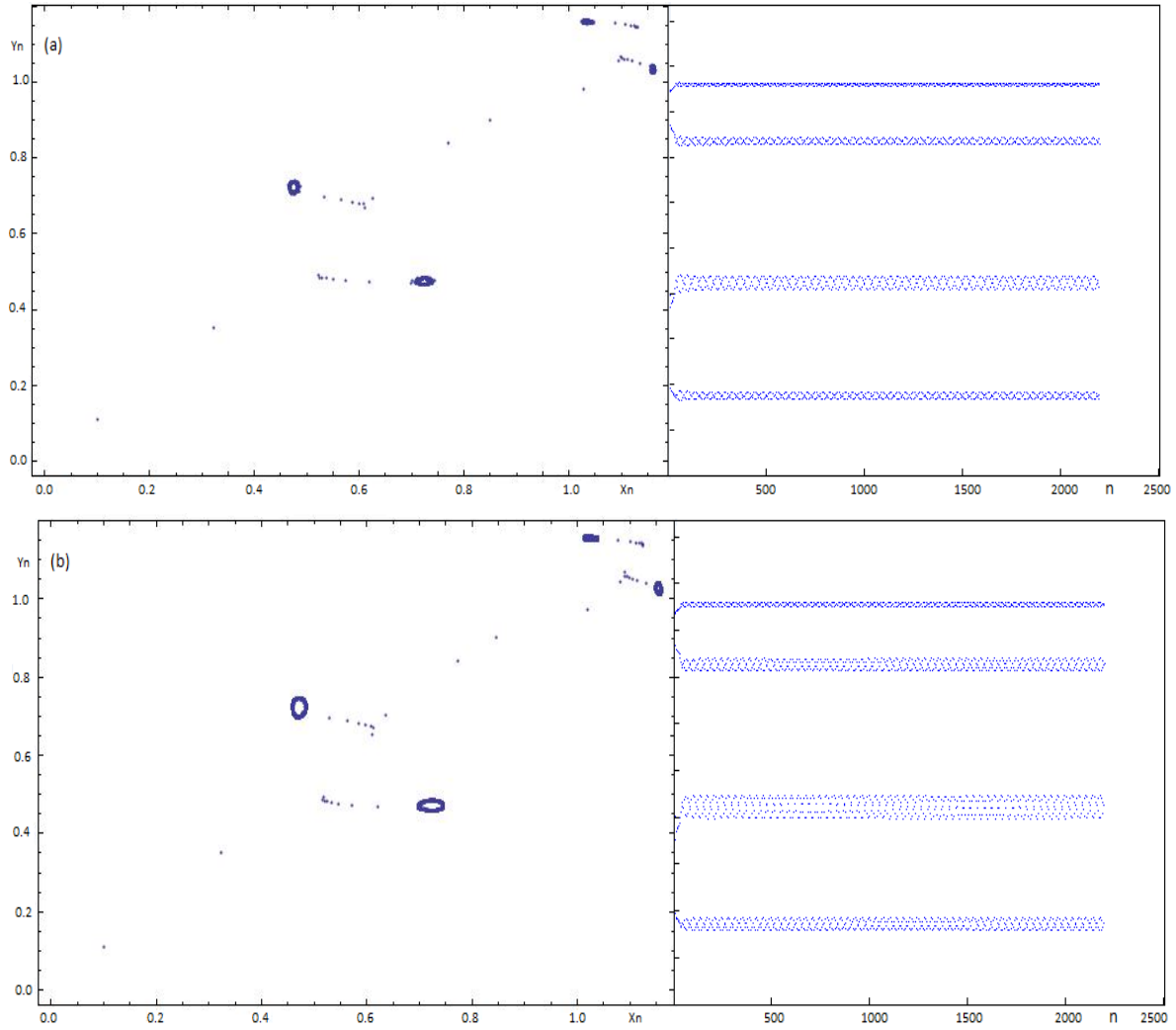

Fig. 4 Phase space (x_n, y_n) is plotted by solving Eq. (24) for $\lambda_1 = \lambda_2 = 1.25$ and (a) $\gamma = 0.1845,$ (b) $\gamma = 0.2.$ Isolated points in (a) and (b) are part of transient evolution. The plots on right hand side shows behavior of our system, which is going from 4P state to chaos through QP in which each attractor shows nine wing pattern as in Fig. 2(a) and fluctuates up to certain values of coupling strength. The attractors expand as a function of increasing coupling strength, γ as shown in Fig. 2(b), corresponding to frequency locking

However, at $\gamma = 0.269$ each period (line) split into eight to four to two and then finally fused in 4P and chaotic attractors remain mirror images to each other, as shown in the Fig. 5(a, b). It has been observed that our coupled nonlinear system got synchronized to each other during these intervals, such that $\gamma \in [0.26, 0.27]$ and $[0.29, 0.30]$ [25, 36]. Chaotic attractors are mirror images of each other in the interval, i. e, $[0.319, 0.445].$ While the trajectory changes at $\gamma = 0.384$ and increases above this value as we get different form of trajectory, i. e, chaotic attractors are not mirror images [29]. The coalesce $(8C \to 4C \to 2C)$ chaos to chaos is analogous to the band emerging in a logistic map [25]. Therefore, periodicity of coupled lasing system oscillates (4P to 32P, each line of period 4 bifurcate then multibifurcation behavior and then converges to 4P at $\gamma = 0.999$) 4P to 8P to 16 to 32P through QP and chaotic and then comes at 4P at last value of and attractors rotate in clockwise direction.

For $\lambda_i = 1.26$ and $\gamma \in [0.001, 0.15]$ it has same behavior as for $\lambda_i = 1.25$ for all values of γ. From $\gamma = 0.152$ to $0.2271,$ the trajectory converges to a periodic solution with the period equal to 4 but strange attractors are not mirror image of each other. However for $\gamma = 0.2275$ to 0.2279 system remains chaotic and then converges to exactly 20 iteration (20P and 20 attractors) at $\gamma = 0.2285.$ Chaoticity and periodicity (20P) oscillate in the interval $[0.2285, 2395]$ and some other complicated phenomena also happened [36]. At $\gamma = 0.2398,$ there exists transient state in which phase space trajectory and periodicity change because of crises as shown in Fig. 6(b). When γ is increased in the interval $[0.295, 0.445]$ having 20P, chaotic behavior through intermittency occurs at $\gamma = 0.449,$ as shown in Fig. 7 and QP at $\gamma = 0.510$ and then converges to 4P at all above values of $\gamma = 0.575.$ Therefore, for this

fixed value of controlling parameters and changing coupling strength our system remains chaotic in between 4P.

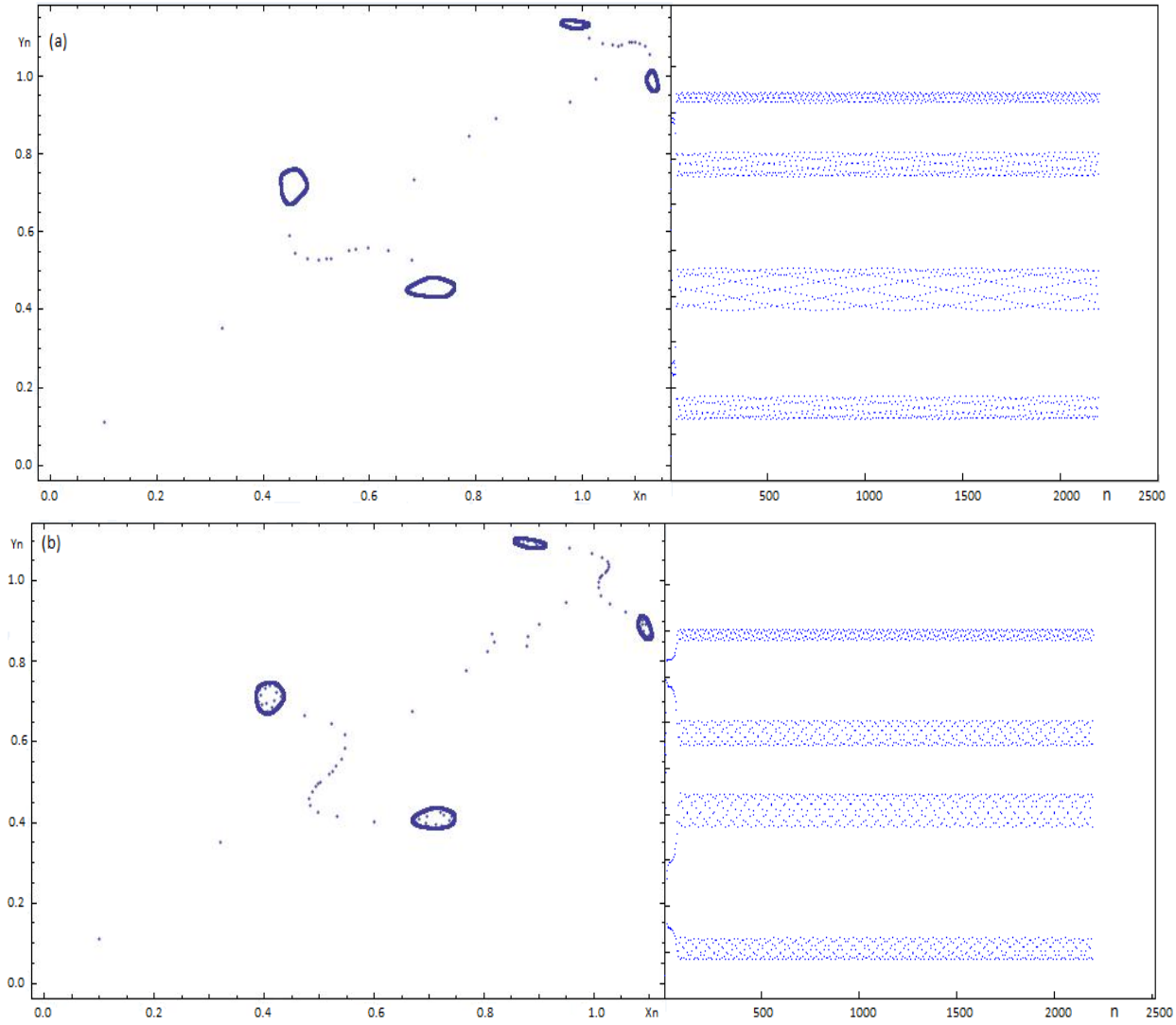

Fig. 5 Phase space (x_n, y_n) is plotted by solving Eq. (24) for $\lambda_1 = \lambda_2 = 1.25$ and (a) $\gamma = 0.2690$, (b) $\gamma = 0.4450$. Our dynamical system is going from unstable state to stable state through QP and trajectory of basin boundary remains invariant after crises. The plots on the right hand side show that (a) there occurs 32P state and (b) QP state after crises

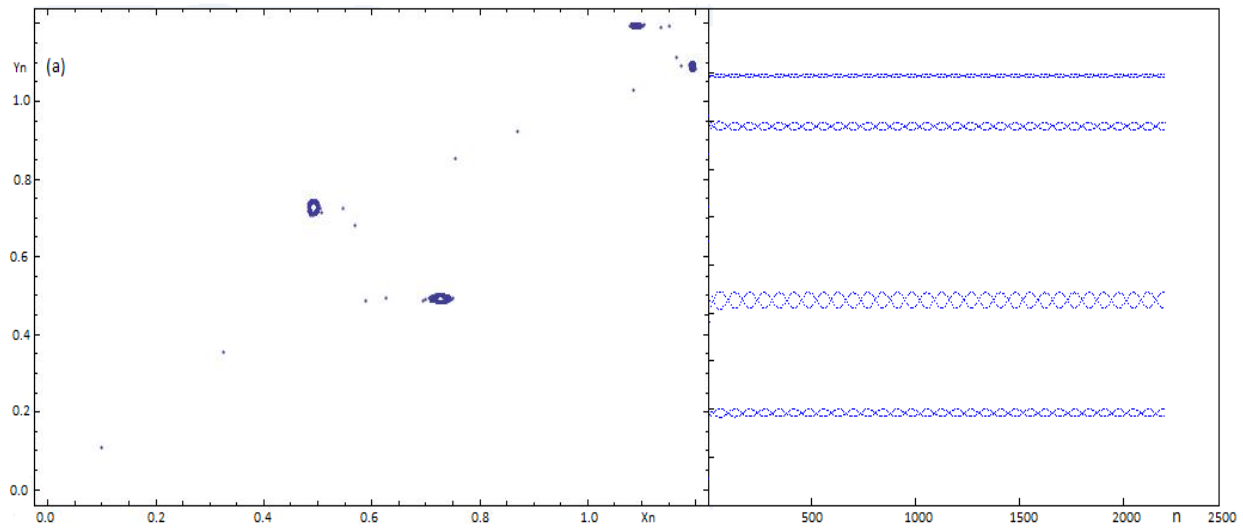

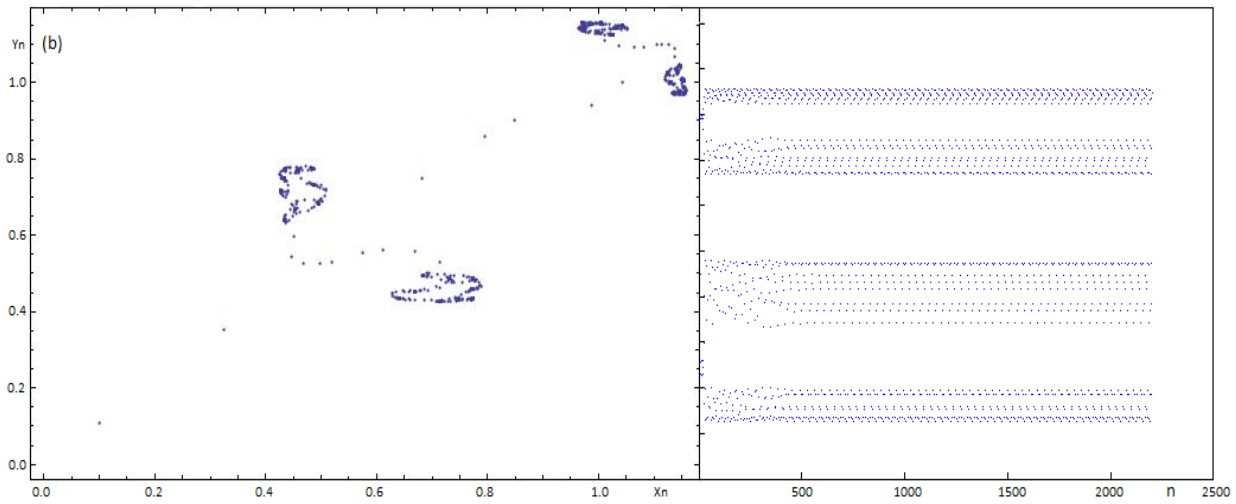

Fig. 6 Phase space (x_n, y_n) is plotted by solving Eq. (24) for $\lambda_1 = \lambda_2 = 1.26$ and (a) $\gamma = 0.09$, (b) $\gamma = 0.2398$. Isolated points in (a) and (b) are part of transient evolution. The plots on the right hand side show behavior of our system that is going from stable state to stability through chaotic and QP states. Here trajectory and periodicity of our system dramatically change because of crises. Here exterior crises is observed between two trajectories

For $\lambda_1 = 1.27$ and $\gamma \in [0.001, 0.011]$ the trajectory in the phase space converges to four strange attractors corresponding to periodicity its asymptotic character of solution is 4P, as shown in the Fig. 8. At the upper range of this interval our system shows chaotic behavior through nodal period, QP and 20P. Lasing system shows chaotic behavior for small interval of time and comes back to its initial state when the coupling strength reaches its maximum value for small values of parameters.

For $\lambda_1 = 1.28$ and in this interval $\gamma \in [0.001, 0.017]$ the trajectory converges to the 8QP or torus corresponding to periodicity it has an 8P asymptotic character of solution. Here, we observe QP (from 8P to 16P) and then (16P to 8P) in the interval $[0.018, 0.0321]$ and then chaotic behavior at $\gamma = 0.045$ through intermittency state at $\gamma = 0.0429$ [37]. From Fig. 9(a), there are 16 chaotic attractors which are not mirror images at $\gamma = 0.0321$ and correspond to intermittence state and show QP after crises, i. e, 16C coalesce into 4T at $\gamma = 0.0445$, which are mirror images as well as synchronized images [16, 26]. Moreover, initially chaos come through QP and intermittency state when system transits from 8P to 16P and after that our system shows chaoticity, but when it returns to its period 16 from chaoticity (infinite periods), no QP and intermittency state is observed up to four decimal places and then periods 8. It is also seen that periodicity, intermittency and chaoticity oscillate in the interval $[0.365, 0.370]$. We observe a transitions from 8P to 4P because of crises at $\gamma = 0.6777$ and then come back to its initial state of 8P at final value of $\gamma = 0.999$ through QP and chaotic states. At the upper range of this interval $\lambda_1 \in [1.29, 1.32]$ our system transits permanently to chaotic regime for all values of coupling strength.

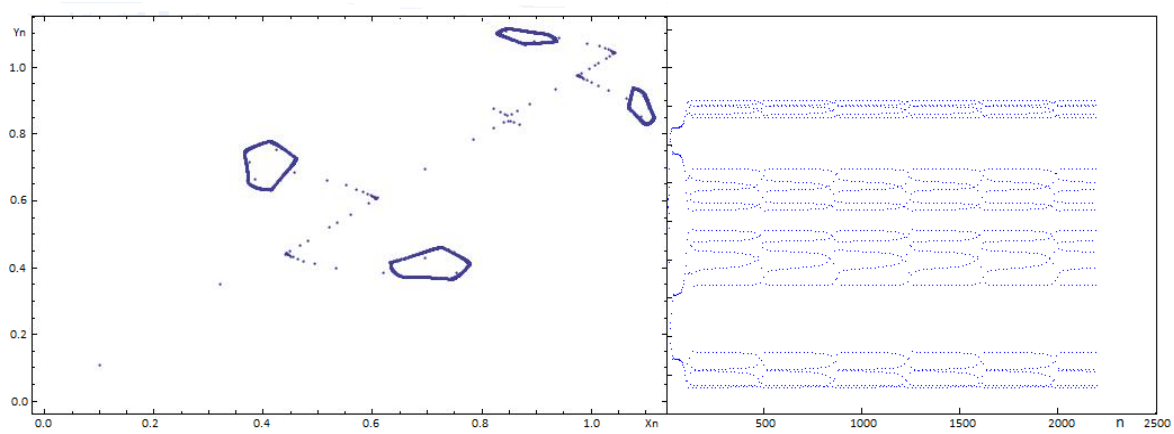

Fig. 7 Phase space (x_n, y_n) is plotted by solving Eq. (24) for $\lambda_1 = \lambda_2 = 1.26$ and $\gamma = 0.4490$. Isolated points are part of transient evolution, intermittency state corresponds to strange at-tractors are synchronized as well as mirror images of each other. The plot on the right side in phase space shows intermittency state in (y; t) plane

Thus, we can say that there exists such type of transition in which we observe "cycle $\rightarrow$ (doubling).... $\rightarrow$ longer cycle $\rightarrow$ Hopf bifurcation $\rightarrow$ torus $\rightarrow$ various frequency locking $\rightarrow$ chaos $\rightarrow$ evolution of chaos $\rightarrow$ chaos (fusion) and then hyperchaos in our system [25]. If one analyzes the two dimensional plots (x_n, y_n) as Poincare surfaces of section for the continuous system, the sequence can be described as: The 2P corresponds to a stable limit cycle. As the increasing further, the limit cycle becomes unstable and bifurcates into a four-loop limit cycle and then evolves into an eight-loop torus through a

Hopf bifurcation. The torus represents quasiperiodic behavior of our system and is responsible for the four invariant orbits on the Poincare surfaces of section. The four intermittency periodic behaviors are obtained when the four characteristic frequencies on the torus are in ratio of two small integers [38]. Higher bifurcation of the torus occurs as the system moves out of quasiperiodic region, by increasing (Ruelle-Takens-Newhouse scenario) [38].

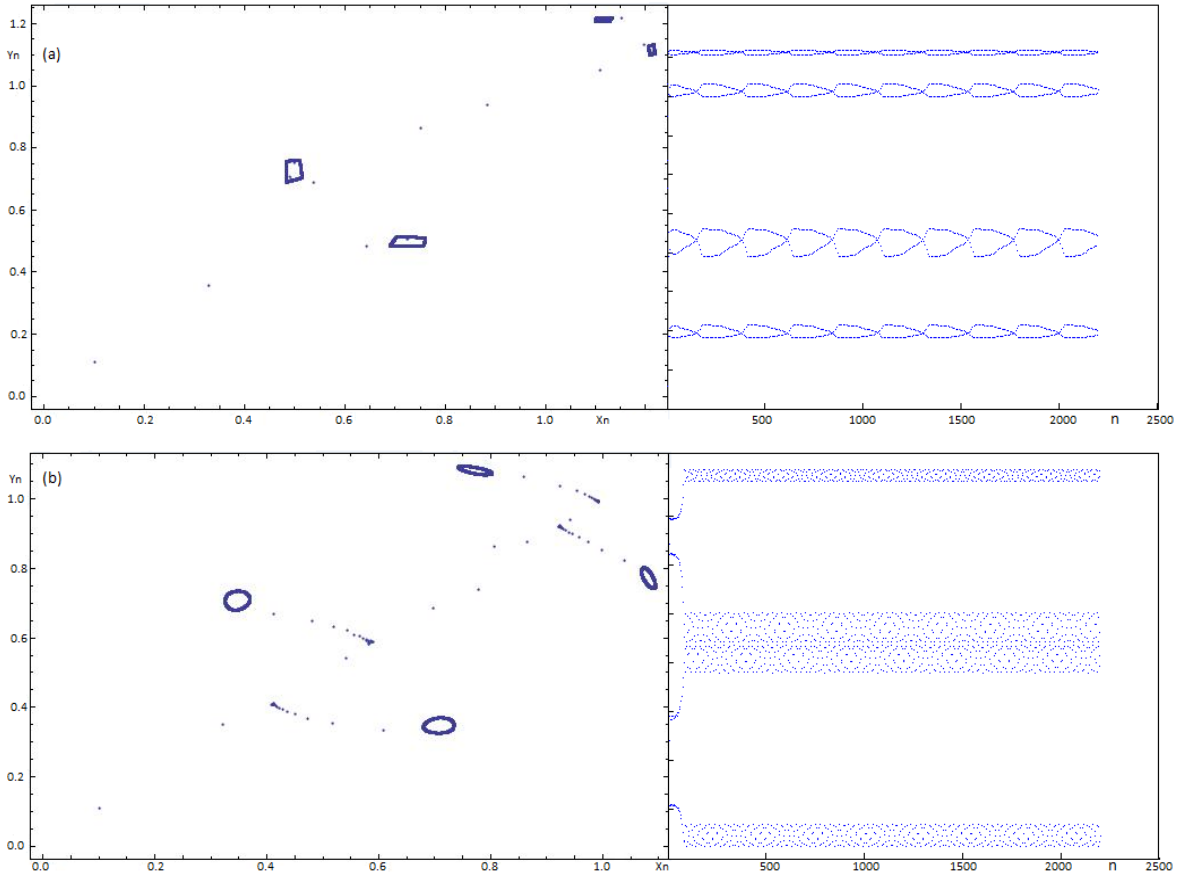

Fig. 8 Phase space (x_n, y_n) is plotted by solving Eq. (24) for $\lambda_1 = \lambda_2 = 1.27$ and (a) $\gamma = 0.045$, (b) $\gamma = 0.6099$. As we mentioned earlier, isolated points in (a) and (b) are part of transient evolution. The plots on the right side of (a) shows stability and (b) shows intermittency state of the system. Therefore, our dynamical system is going from stable state to unstable state through QP because of crises

When λ_1 and λ_2 are not equal to each other then irregular behaviors displayed by means of period doubling bifurcation [38]. But in our dynamical system we have in region for which, start at same values for $\gamma = 0.051$. If γ is fixed and λ_i is varied from 1.5 to 4, we have detected period doubling bifurcation which leads to 64P solutions and then to chaos. Thus, from the above two cases we conclude that when $\lambda_1 = \lambda_2$ and variation exist in γ, chaos emerges through quasiperiodicity, however, when $\lambda_1 \neq \lambda_2$, chaos emerges by mean of period doubling bifurcation sequence.

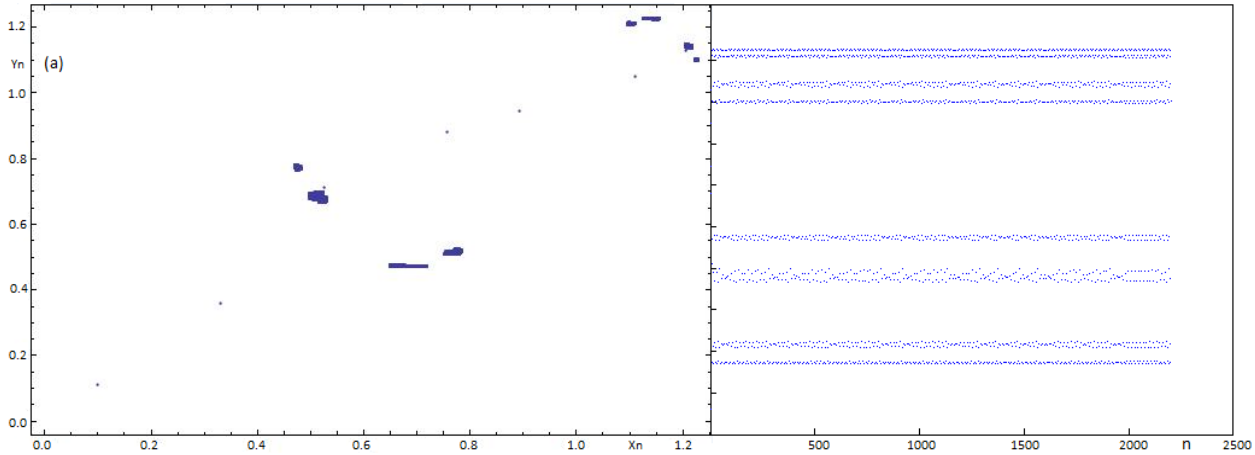

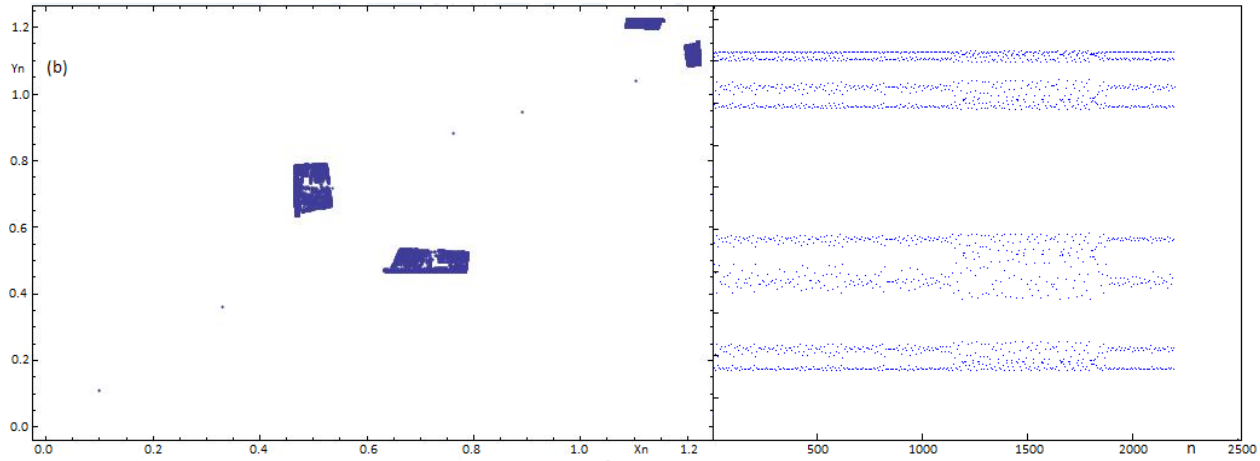

Fig. 9 Phase space (x_n, y_n) is plotted by solving Eq. (24) for $\lambda_1 = \lambda_2 = 1.28$ and (a) $\gamma = 0.0321$, (b) $\gamma = 0.0445$. The plots on the right hand side show our system is going from unstable state to stable state through chaotic and QP states

VI. CONCLUSIONS

In this paper we analyze the nonlinear evolution of laser light in semi-classical and quantum mechanical domains and consequently explain the interaction of atoms with the field in a ring cavity. We report that LLM displays characteristics, such as, convergence, cyclic, and chaotic behavior, as a function of controlling parameter *r* which helps to identify different behaviors of lasers in a ring cavity. As an important result, we describe bistability and entanglement with the help of cyclic solution or bifurcation of LLM. In general, we discuss the stable, bistable/multi bistable and chaotic laser in a ring cavity. The Feigenbaum number is evaluated for our system to describe chaotic laser light. The coupling between two laser logistic equations has a profound effect on the character of solutions and approach to chaos that is observed for one dimensional logistic map.

We here also provide detailed study of transition from stability to chaos and torus to chaos in two dimensional mapping. It is seen that transition from periodicity (stability) and quasiperiodicity (torus) to chaos occurs with frequency locking. Through our numerical calculations for two-mode ring lasers, we have concluded following points: (i) Torus appears by way of Hopf bifurcation; (ii) Shape of strange attractors changes as controlling parameter changes or torus is distorted as change. At certain values they expand and after that reduce in size; (iii) Chaos appears through a period-doubling bifurcation of some frequency-locked cycle at some values of the bifurcation parameter; (iv) Our dynamical system oscillate from 2P to 4P and then 4P to 2P through quasi-periodicity and intermittency state, at $\lambda_i \in [0.25, 1.23]$ and for all values of $\gamma \in [0.001, 0.999]$; (v) Above this value of λ_i our system shows random behaviors through QP and some other complicated states. At some place we get periodicity and then chaoticity and then again periodicity not through QP but direct change of the state; (vi) Synchronization is destroyed and reinforced due to crises, corresponding to change of the coupling parameter. There are two pairs of laser attractors in phase space, which are totally different from each other at certain values of parameters, whereas synchronized as well as mirror images are the same of each other at other values of characteristic parameters. For $\lambda_i = 1.26$ and $\gamma \in [0.001, 0.051]$ they display approximately same behavior as mentioned above, the difference is that it remains chaotic at $\gamma = 0.2279$ and obtains asymptotic solution of 20P at $\gamma = 0.2285$. Therefore, our dynamical system shows periodicity, quasiperiodicity, intermittency state to chaotic, to periodic state and then shows permanently chaotic behavior at $\lambda_i = 1.3$ and all higher values, and for all positive values of $\gamma \in [0.001, 0.999]$. In coupled laser logistic equations, periodicity changes during frequency locking because of interior crises.

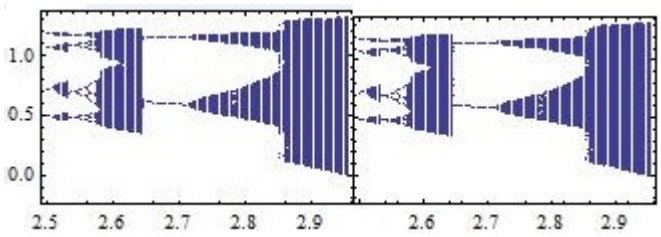

Fig. 10 Bifurcation diagram for the coupled lasers Eq. (24) for $\lambda_1 = \lambda_2 = 1.5$ range from 2.5 to 2.9 and $\gamma = 0.051$. . For each value of λ_i we used the final point of the previous λ_i value and 1600 iterates are plotted. This shows the period-doubling sequence as well as QP and chaotic regions

REFERENCES

[1] W. E. Lamb, Phy. Rev. 134, 1429. (1965).

[2] H. Haken., "Analogy between higher instabilities in fluids and lasers," Phys. Lett. A 53, 77 (1975).

[3] M. I. Rabinovich, "Stochastic auto oscillations and turbulence," Usp. Fiz. Nauk. 125, 123 (1978).

[4] T. Yamada, and R. Graham, "Chaos in a Laser System under a Modulated External Field," Phys. Rev. Lett. 45, 1322 (1980).

[5] A. C. Newell, and Moleny. J. V, "*Nonlinear Optics,"* Addison-Wesley publishing Company, 1991); F. Saif, Fam Le Kien, and M. S. Zubairy, "Quantum theory of a micromaser operating on the atomic scattering from a resonant standing wave" Physical Review A 64 , 043812 (2001).

[6] R. M May, "Simple mathematical models with very complicated dynamics," Nature 261, 459 (1976).

[7] J. R. Beddington, C. A. Free and J. H. Lawton, "Characteristics of successful natural enemies in models of biological control of insect pests," Nature (London), 58, 255 (1975).

[8] R. C. Hilborn, "Chaos and Nonlinear Dynamics: An Introduction for Scientists and Engineers," (Oxford University Press, USA, 2001).

[9] R. Blumel, and W. P. Reinhardt, "Chaos in Atomic Physics*,"* (Cambridge University Press, Cambridge, (1997). Farhan Saif "Quantum Recurrences: A probe to study Quantum Chaos" Physical Review E 62, 6308 (2000). Farhan Saif, 'Classical and Quantum Chaos in Atom Optics', Physics Reports 419, 207 (2005).

[10] K. Kaneko, "Transition from Torus to Chaos Accompanied by Frequency Lockings with Symmetry Breaking," Prog. Theor. Phys. 69, 1427 (1983).

[11] John Vandermeer and Andrew Kaufmann, "Models of coupled population oscillators using 1-D maps," Journal of Mathematical Biology 37, 178 (1998).

[12] A. Hohl, A. Gavrielides, T. Erneux, and V. Kovanis, "Localized Synchronization in Two Coupled Nonidentical Semiconductor Lasers," Phys. Rev. Lett. 78, 25 (1997).

[13] C. Cohen-Tannoudji, B. Diu, and F. Lalöe, "Quantum Mechanics*,"* (Johan Wiley and Sons, New York 1977).

[14] B. W. Shore, "The Theory of Coherent atomic excitation*,"* (John Wiley and Sons Inc, 1989).

[15] M. Sargent, M. O. Scully, and E. Lamb, "Elements of Quantum Optics," (Springer-Verlag Berlin Heidelberg, Reading Mass, 2007).

[16] M. O. Scully and M. S. Zubairy, "Quantum Optics*,"* (Cambridge University Press, 1997).

[17] W. T. Silfast, "Laser Fundamentals Second Edition," (Cambridge University Press, Cambridge, 2004).

[18] M. Mandel and E.Wolf, "Optical Coherence and Quantum Optics*,"* (Cambridge University Press, Cambridge, 1995).

[19] M. M. Tehrani and L. Mandel, "Mode coupling and detunning in a ring laser,"Opt. Commun. 16, 16 (1976).

[20] Herbert G. Winful and L. Rahman, "Synchronized chaos and spatiotemporal chaos in arrays of coupled lasers," Phys. Rev. Lett. 65, 1575–1578 (1990).

[21] A. Englert, S. Heiligenthal, W. Kinzel and I. Kanter, "Synchronization of chaotic networks with time-delayed couplings: An analytic study,"Phys. Rev. E. 83, 046222 (2011).

[22] Shuguang Guan, G. W. Wei, and C. H Lai, "Controllability of flow turbulence," Phys. Rev. E. 69, 066214 (2004).

[23] Sudeshna Sinha , "Random coupling of chaotic maps leads to spatiotemporal synchronization," Phy. Rev. E 66, 016209 (2008).

[24] M. Abdul and F. Saif, Appl. Math. Inf. Sci. 6, No. 1, 29-33 (2012). M. Abdul and Farhan Saif, "Synchronized Attractors and entrained Chaos" in Proceedings of International Multi-Conference of Engineers and Computer Scientists, 11-14 June, p. 90-97 (2013).

[25] K. Kaneko, "Transition from Torus to Chaos Accompanied by Frequency Lockings with Symmetry Breaking," Progress of Theoretical Physics 69, 1427 (1983).

[26] G. Tanaka, M. A. F. Sanjun, and K. Aihara, "Crisis-induced intermittency in two coupled chaotic maps: Towards understanding chaotic itinerancy," Phys. Rev. E. 71, 016219 (2005).

[27] S. Wiggins, "Global Bifurcations and Chaos: Analytical Methods," New York: Springer-Verlag, New York, (1988).

[28] Parker. T. S and L. O. Chua, "Practical Numerical Algorithms for Chaotic System," New York: Springer-Verlag, New York, (1989).

[29] A. Garnkel, "Self-organizing systems," (Plenum Press, New York, 1987).

[30] J. Briggs, and F. D. Peat, "The turbulent mirror," Harper and Row Press, New York, (1989).

[31] O. E. Rossler, "The chaotic hierarchy. In A Chaotic Hi-erarchy", Singapore, (1991).

[32] R. Blumel, and W. P. Reinhardt, "Chaos in Atomic Physics," Cambridge University Press, Cambridge, (1997).

[33] C. Grebogi, E. Ott and J. A. Yorke, "Chaotic Attractors in Crisis," Phys. Rev. Lett. 48, 1507 (1982).

[34] Xingyuan. Wang and Chao Luo, Inter. Jour. of Mode. Phys. B. 22, 427 (2008).

[35] V. Astakhov, A. Shabunin, T. Kapitaniak and V. An-ishchenko, "Loss of Chaos Synchronization through the Sequence of Bifurcations of Saddle Periodic Orbits," Phys. Rev. L. 79, 1014–1017 (1997).

[36] V. Astakhov, A Shabunin, W. Uhm and S. Kim, "Multistability formation and synchronization loss in coupled Hénon maps: Two sides of the single bifurcational mechanism,"Phys. Rev. E. 63, 056212 (2001).

[37] Arne Jakobsen , "Symmetry breaking bifurcation in a circular chain of N coupled logistic maps," Physica. D 237, 3382 (2008).

[38] Zhanybai T. Zhusubaliyev, and E. Mosekilde, "Multilayered tori in a system of two coupled logistic maps," Phys. Lett. A. 373, 946 (2011).

[39] J. M. Yuan, M. Tung, D. H. Feng, and L. M. Narducci, "Instability and irregular behavior of coupled logistic equations," Phys. Rev. A. 28, 1662 (1983). Edson D. Leonel, Juliano A. de Oliveira, Farhan Saif, "Critical exponents for transition from integrability to non-integrability via localization of invariant tori in Hamiltonian systems" Journal of Physics A: Mathematical and Theoretical 44(30), 302001 (2011).

Muhammad Abdul is a Research Associate at the Department of Electronics, Quaid-i-Azam University, Islamabad Pakistan. He is also a research fellow in the HEC research project "Nano Device: Theoretical, Experimental and Technological Implementations". His main areas of research include Quantum Information, Quantum Optics, Quantum Chaos, Condense Matter Physics and Medical Engineering.

Umar F. Zubairy is a doctorate student at the University of Camerino, Italy. He is a previous research associate at the Quantum Electronics Labs (QUELL), Department of Electronics, Quaid-i-Azam University, Islamabad Pakistan. He is also a research fellow in the HEC research project "Nano Device: Theoretical, Experimental and Technological Implementations". His main areas of research include Quantum Information, Quantum Optics, and Classical Chaos.

Farhan Saif is chairman Department of Electronics Quaid-I-Azam University Islamabad and Ex-Head of the Department, Centre for Advanced Mathematics and Physics, NUST and Principle Researcher, Quantum Electronics Labs (QUELL), Department of Electronics, Quaidi-Azam University, Islamabad, Pakistan. In his research work he has invented Recurrence Tracking Microscope as a novel technique to scan nano-structures, nano sensors to calculate mass, gravity, time and position with better accuracy. His main research areas include Bose-Einstein Condensation, Nano Science and Technology, Quantum Informatics, Quantum metrology, MatterWave Optics, Classical/Quantum Chaos. He has also presented numerous techniques to engineer Universal quantum logic gates and various kind of entanglement in various cavity QED setups. In addition Dr. Saif has published more than eighty-five research articles in international journals, which have been highly cited by reputed authors and researchers. In addition he presented his work in all the continents of the world as invited speaker and visiting professor. He is collaborating with University of Ulm, Germany, University of Sao Paulo, Brazil, University of Electro-Communications, Japan, University of Arizona, USA.